Determination of f_s/f_d for 7 TeV pp Collisions and Measurement of the $B^0 \to D^- K^+$ Branching Fraction

R. Aaij *et al.**
(LHCb Collaboration)
(Received 28 June 2011; published 14 November 2011)

The relative abundance of the three decay modes $B^0 \to D^- K^+$, $B^0 \to D^- \pi^+$, and $B_s^0 \to D_s^- \pi^+$ produced in 7 TeV pp collisions at the LHC is determined from data corresponding to an integrated luminosity of 35 pb^{-1}. The branching fraction of $B^0 \to D^- K^+$ is found to be $\mathcal{B}(B^0 \to D^- K^+) = (2.01 \pm 0.18^{\mathrm{stat}} \pm 0.14^{\mathrm{syst}}) \times 10^{-4}$. The ratio of fragmentation fractions f_s/f_d is determined through the relative abundance of $B_s^0 \to D_s^- \pi^+$ to $B^0 \to D^- K^+$ and $B^0 \to D^- \pi^+$, leading to $f_s/f_d = 0.253 \pm 0.017 \pm 0.017 \pm 0.020$, where the uncertainties are statistical, systematic, and theoretical, respectively.

DOI: 10.1103/PhysRevLett.107.211801 PACS numbers: 13.25.Hw, 12.38.Qk, 13.60.Le, 13.87.Fh

Knowledge of the production rate of B_s^0 mesons is required to determine any B_s^0 branching fraction. This rate is determined by the $b\bar{b}$ production cross section and the fragmentation probability f_s, which is the fraction of B_s^0 mesons among all weakly decaying bottom hadrons. Similarly, the production rate of B^0 mesons is driven by the fragmentation probability f_d. The measurement of the branching fraction of the rare decay $B_s^0 \to \mu^+\mu^-$ is a prime example where improved knowledge of f_s/f_d is needed to reach the highest sensitivity in the search for physics beyond the standard model [1]. The ratio f_s/f_d is, in principle, dependent on collision energy and type as well as the acceptance region of the detector. This is the first measurement of this quantity at the LHC.

The ratio f_s/f_d can be extracted if the ratio of branching fractions of B^0 and B_s^0 mesons decaying to particular final states X_1 and X_2, respectively, is known:

$$\frac{f_s}{f_d} = \frac{N_{X_2}}{N_{X_1}} \frac{\mathcal{B}(B^0 \to X_1)}{\mathcal{B}(B_s^0 \to X_2)} \frac{\epsilon(B^0 \to X_1)}{\epsilon(B_s^0 \to X_2)}. \tag{1}$$

The ratio of the branching fraction of the $B_s^0 \to D_s^- \pi^+$ and $B^0 \to D^- K^+$ decays is dominated by contributions from color-allowed tree-diagram amplitudes and is therefore theoretically well understood. In contrast, the ratio of the branching ratios of the two decays $B_s^0 \to D_s^- \pi^+$ and $B^0 \to D^- \pi^+$ can be measured with a smaller statistical uncertainty due to the greater yield of the B^0 mode but suffers from an additional theoretical uncertainty due to the contribution from a W-exchange diagram. Both ratios are exploited here to measure f_s/f_d according to the equations [2,3]

$$\frac{f_s}{f_d} = 0.971 \left|\frac{V_{us}}{V_{ud}}\right|^2 \left(\frac{f_K}{f_\pi}\right)^2 \frac{\tau_{B_d}}{\tau_{B_s}} \frac{1}{\mathcal{N}_a \mathcal{N}_F} \frac{\epsilon_{D^- K^+}}{\epsilon_{D_s^- \pi^+}} \frac{N_{D_s^- \pi^+}}{N_{D^- K^+}} \tag{2}$$

and

$$\frac{f_s}{f_d} = 0.982 \frac{\tau_{B_d}}{\tau_{B_s}} \frac{1}{\mathcal{N}_a \mathcal{N}_F \mathcal{N}_E} \frac{\epsilon_{D^- \pi^+}}{\epsilon_{D_s^- \pi^+}} \frac{N_{D_s^- \pi^+}}{N_{D^- \pi^+}}. \tag{3}$$

Here ϵ_X is the selection efficiency of decay X (including the branching fraction of the D decay mode used to reconstruct it), N_X is the observed number of decays of this type, the V_{ij} are elements of the Cabibbo-Kobayashi-Maskawa matrix, f_i are the meson decay constants, and the numerical factors take into account the phase space difference for the ratio of the two decay modes. Inclusion of charge conjugate modes is implied throughout. The term $\mathcal{N}_a$ parametrizes nonfactorizable $SU(3)$-breaking effects; $\mathcal{N}_F$ is the ratio of the form factors; $\mathcal{N}_E$ is an additional correction term to account for the W-exchange diagram in the $B^0 \to D^- \pi^+$ decay. Their values [2,3] are $\mathcal{N}_a = 1.00 \pm 0.02$, $\mathcal{N}_F = 1.24 \pm 0.08$, and $\mathcal{N}_E = 0.966 \pm 0.075$. The latest world average [4] is used for the B meson lifetime ratio $\tau_{B_s}/\tau_{B_d} = 0.973 \pm 0.015$. The numerical values used for the other factors are $|V_{us}| = 0.2252$, $|V_{ud}| = 0.97425$, $f_\pi = 130.41$, and $f_K = 156.1$, with negligible associated uncertainties [5].

The observed yields of these three decay modes in 35 pb^{-1} of data collected with the LHCb detector in the 2010 running period are used to measure f_s/f_d averaged over the LHCb acceptance and to improve the current measurement of the branching fraction of the $B^0 \to D^- K^+$ decay mode [6].

The LHCb experiment [7] is a single-arm spectrometer, designed to study B decays at the LHC, with a pseudorapidity acceptance of $2 < \eta < 5$ for charged tracks. The first trigger level allows the selection of events with B hadronic decays using the transverse energy of hadrons measured in the calorimeter system. The event information

*Full author list given at the end of the article.

is subsequently sent to a software trigger, implemented in a dedicated processor farm, which performs a final online selection of events for later offline analysis. The tracking system determines the momenta of B decay products with a precision of $\delta p/p = 0.35\%$–0.5%. Two ring imaging Cherenkov detectors allow charged kaons and pions to be distinguished in the momentum range 2–100 GeV/c [8].

The three decay modes $B^0 \to D^-(K^+\pi^-\pi^-)\pi^+$, $B^0 \to D^-(K^+\pi^-\pi^-)K^+$, and $B_s^0 \to D_s^-(K^+K^-\pi^-)\pi^+$ are topologically identical and can therefore be selected by using identical geometric and kinematic criteria, thus minimizing efficiency differences between them. Events are selected at the first trigger stage by requiring a hadron with transverse energy greater than 3.6 GeV in the calorimeter. The second, software, stage [9,10] requires a two-, three-, or four-track secondary vertex with a high sum p_T of the tracks, significant displacement from the primary interaction, and at least one track with exceptionally high p_T, large displacement from the primary interaction, and small fit χ^2.

The decays of B mesons can be distinguished from the background by using variables such as the p_T and impact parameter χ^2 of the B, D, and the final state particles with respect to the primary interaction. In addition, the vertex quality of the B and D candidates, the B lifetime, and the angle between the B momentum vector and the vector joining the B production and decay vertices are used in the selection. The D lifetime and flight distance are not used in the selection because the lifetimes of the D_s^- and D^- differ by about a factor of 2.

The event sample is first selected by using the gradient boosted decision tree technique [11], which combines the geometrical and kinematic variables listed above. The selection is trained on a mixture of simulated $B^0 \to D^-\pi^+$ decays and combinatorial background selected from the sidebands of the data mass distributions. The distributions of the input variables for data and simulated signal events show excellent agreement, justifying the use of simulated events in the training procedure.

Subsequently, D^- (D_s^-) candidates are identified by requiring the invariant mass under the $K\pi\pi$ ($KK\pi$) hypothesis to fall within the selection window 1870^{+24}_{-40} (1969^{+24}_{-40}) MeV/c^2, where the mass resolution is approximately 10 MeV/c^2. The final $B^0 \to D^-\pi^+$ and $B_s^0 \to D_s^-\pi^+$ subsamples consist of events that pass a particle identification (PID) criterion on the bachelor particle, based on the difference in log-likelihood between the charged pion and kaon hypotheses (DLL) of $\mathrm{DLL}(K-\pi) < 0$, with an efficiency of 83.0%. The $B^0 \to D^-K^+$ subsample consists of events with $\mathrm{DLL}(K-\pi) > 5$, with an efficiency of 70.2%. Events not satisfying either condition are not used.

The relative efficiency of the selection procedure is evaluated for all decay modes using simulated events, where the appropriate resonances in the charm decays are taken into account. As the analysis is sensitive only to relative efficiencies, the impact of differences between the data and simulation is small. The relative efficiencies are $\epsilon_{D^-\pi^+}/\epsilon_{D^-K^+} = 1.221 \pm 0.021$, $\epsilon_{D^-K^+}/\epsilon_{D_s^-\pi^+} = 0.917 \pm 0.020$, and $\epsilon_{D^-\pi^+}/\epsilon_{D_s^-\pi^+} = 1.120 \pm 0.025$, where the errors are due to the limited size of the simulated event samples.

The relative yields of the three decay modes are extracted from unbinned extended maximum likelihood fits to the mass distributions shown in Fig. 2. The signal mass shape is described by an empirical model derived from simulated events. The mass distribution in the simulation exhibits non-Gaussian tails on either side of the signal. The tail on the right-hand side is due to non-Gaussian detector effects and modeled with a crystal ball function [12]. A similar tail is present on the left-hand side of the peak. In addition, the low mass tail contains a second contribution due to events where hadrons have radiated photons that are not reconstructed. The sum of these contributions is modeled with a second crystal ball function. The peak values of these two crystal ball functions are constrained to be identical.

Various backgrounds have to be considered, in particular, the cross feed between the D^- and D_s^- channels, and the contamination in both samples from $\Lambda_b \to \Lambda_c^+\pi^-$ decays, where $\Lambda_c^+ \to pK^-\pi^+$. The D_s^- contamination in the D^- data sample is reduced by loose PID requirements, $\mathrm{DLL}(K-\pi) < 10$ (with an efficiency of 98.6%) and $\mathrm{DLL}(K-\pi) > 0$ (with an efficiency of 95.6%), for the pions and kaons from D decays, respectively. The resulting efficiency to reconstruct $B_s^0 \to D_s^-\pi^+$ as background is evaluated, by using simulated events, to be 30 times smaller than for $B^0 \to D^-\pi^+$ and 150 times smaller than for $B^0 \to D^-K^+$ within the B^0 and D^- signal mass windows. By taking into account the lower production fraction of B_s^0 mesons, this background is negligible.

The contamination from Λ_c decays is estimated in a similar way. However, different approaches are used for the B^0 and B_s^0 decays. A contamination of approximately 2% under the $B^0 \to D^-\pi^+$ mass peak and below 1% under the $B^0 \to D^-K^+$ peak is found, and therefore no explicit $\mathrm{DLL}(p-\pi)$ criterion is needed. The Λ_c background in the B_s^0 sample is, on the other hand, large enough that it can be fitted for directly.

A prominent peaking background to $B^0 \to D^-K^+$ is $B^0 \to D^-\pi^+$, with the pion misidentified as a kaon. The small $\pi \to K$ misidentification rate (of about 4%) is compensated by the larger branching fraction, resulting in similar event yields. This background is modeled by obtaining a clean $B^0 \to D^-\pi^+$ sample from the data and reconstructing it under the $B^0 \to D^-K^+$ mass hypothesis. The resulting mass shape depends on the momentum distribution of the bachelor particle. The momentum distribution after the $\mathrm{DLL}(K-\pi) > 5$ requirement can be found by considering the PID performance as a function of momentum. This is obtained by using a sample of $D^{*+} \to D^0\pi^+$ decays and is illustrated in Fig. 1. The mass distribution is reweighted by using this momentum distribution to reproduce the $B^0 \to D^-\pi^+$ mass shape following the DLL cut.

The combinatorial background consists of events with random pions and kaons, forming a fake D^- or D_s^- candidate, as well as real D^- or D_s^- mesons that combine with a random pion or kaon. The combinatorial background is modeled with an exponential shape.

Other background components originate from partially reconstructed B^0 and B_s^0 decays. In $B^0 \to D^-\pi^+$, these originate from $B^0 \to D^{*-}\pi^+$ and $B^0 \to D^-\rho^+$ decays, which can also be backgrounds for $B^0 \to D^-K^+$ in the case of a misidentified bachelor pion. In $B^0 \to D^-K^+$, there is additionally background from $B^0 \to D^{*-}K^+$ decays. The invariant mass distributions for the partially reconstructed and misidentified backgrounds are taken from large samples of simulated events, reweighted according to the mass hypothesis of the signal being fitted and the DLL cuts.

For $B_s^0 \to D_s^-\pi^+$, the $B^0 \to D^-\pi^+$ background peaks under the signal with a similar shape. In order to suppress this peaking background, PID requirements are placed on both kaon tracks. The kaon which has the same sign in the $B_s^0 \to D_s^-\pi^+$ and $B^0 \to D^-\pi^+$ decays is required to satisfy $\mathrm{DLL}(K-\pi) > 0$, while the other kaon in the D_s^+ decay is required to satisfy $\mathrm{DLL}(K-\pi) > 5$. Because of the similar shape, a Gaussian constraint is applied to the yield of this background. The central value of this constraint is computed from the $\pi \to K$ misidentification rate. The $\Lambda_b \to \Lambda_c^+\pi^-$ background shape is obtained from simulated events, reweighted according to the PID efficiency, and the yield allowed to float in the fit. Finally, the relative size of the $B_s^0 \to D_s^-\rho^+$ and $B_s^0 \to D_s^{*-}\pi^+$ backgrounds is constrained to the ratio of the $B^0 \to D^-\rho^+$ and $B^0 \to D^{*-}\pi^+$ backgrounds in the $B^0 \to D^-\pi^+$ fit, with an uncertainty of 20% to account for potential $SU(3)$ symmetry breaking effects.

The free parameters in the likelihood fits to the mass distributions are the event yields for the different event types, i.e., the combinatorial background, partially reconstructed background, misidentified contributions, and the signal, as well as the peak value of the signal shape. In addition, the combinatoric background shape is left free in the $B^0 \to D^-\pi^+$ and $B_s^0 \to D_s^-\pi^+$ fits, and the signal width is left free in the $B^0 \to D^-\pi^+$ fit. In the $B_s^0 \to D_s^-\pi^+$ and $B^0 \to D^-K^+$ fits, the signal width is fixed to the value from the $B^0 \to D^-\pi^+$ fit, corrected by the ratio of the signal widths for these modes in simulated events.

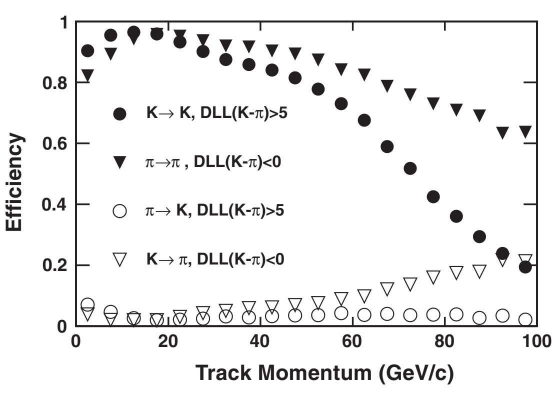

FIG. 1. Probability, as a function of momentum, to correctly identify (full symbols) a kaon or a pion when requiring $\mathrm{DLL}(K-\pi) > 5$ or $\mathrm{DLL}(K-\pi) < 0$, respectively. The correspondent probability to wrongly identify (open symbols) a pion as a kaon, or a kaon as a pion, is also shown. The data are taken from a calibration sample of $D^* \to D(K\pi)\pi$ decays; the statistical uncertainties are too small to display.

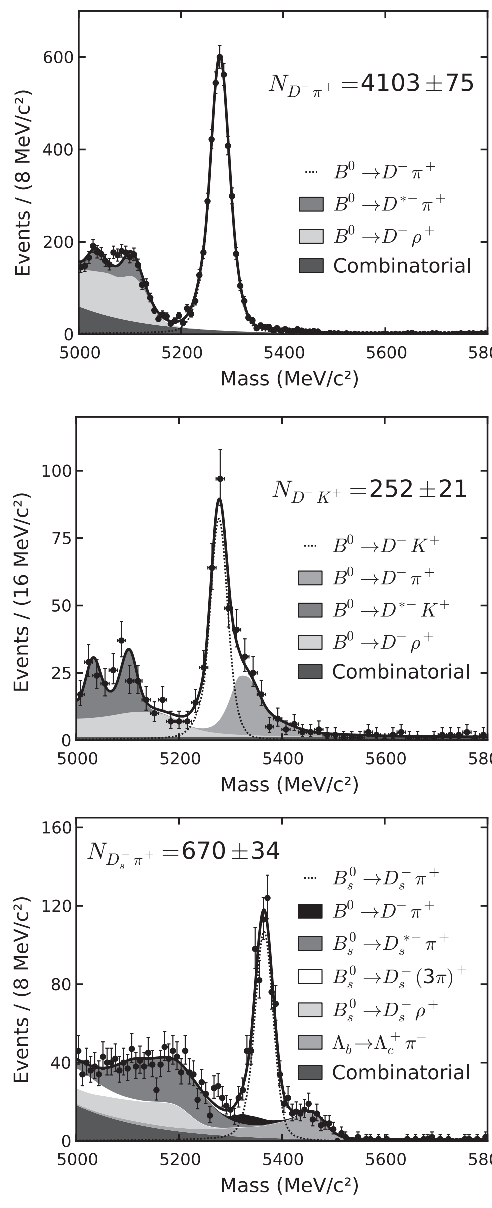

FIG. 2. Mass distributions of the $B^0 \to D^-\pi^+$, $B^0 \to D^-K^+$, and $B_s^0 \to D_s^-\pi^+$ candidates (top to bottom). The indicated components are described in the text.

The fits to the full $B^0 \to D^- \pi^+$, $B^0 \to D^- K^+$, and $B_s^0 \to D_s^- \pi^+$ data samples are shown in Fig. 2. The resulting $B^0 \to D^- \pi^+$ and $B^0 \to D^- K^+$ event yields are 4103 ± 75 and 252 ± 21, respectively. The number of misidentified $B^0 \to D^- \pi^+$ events under the $B^0 \to D^- K^+$ signal as obtained from the fit is 131 ± 19. This agrees with the number expected from the total number of $B^0 \to D^- \pi^+$ events, corrected for the misidentification rate determined from the PID calibration sample, of 145 ± 5. The $B_s^0 \to D_s^- \pi^+$ event yield is 670 ± 34.

The stability of the fit results has been investigated by using different cut values for both the PID requirement on the bachelor particle and for the multivariate selection variable. In all cases, variations are found to be small in comparison to the statistical uncertainty.

The relative branching fractions are obtained by correcting the event yields by the corresponding efficiency factors; the dominant correction comes from the PID efficiency. The dominant source of systematic uncertainty is the knowledge of the $B^0 \to D^- \pi^+$ branching fraction (for the $B^0 \to D^- K^+$ branching fraction measurement) and the knowledge of the D^- and D_s^- branching fractions (for the f_s/f_d measurement). An important source of systematic uncertainty is the knowledge of the PID efficiency as a function of momentum, which is needed to reweight the mass distribution of the $B^0 \to D^- \pi^+$ decay under the kaon hypothesis for the bachelor track. This enters in two ways: first as an uncertainty on the correction factors and second as part of the systematic uncertainty, since the shape for the misidentified backgrounds relies on correct knowledge of the PID efficiency as a function of momentum.

The performance of the PID calibration is evaluated by applying the same method from the data to simulated events, and the maximum discrepancy found between the calibration method and the true misidentification is attributed as a systematic uncertainty. The f_s/f_d measurement using $B^0 \to D^- K^+$ and $B_s^0 \to D_s^- \pi^+$ is more robust against PID uncertainties, since the final states have the same number of kaons and pions.

Other systematic uncertainties are due to limited simulated event samples (affecting the relative selection efficiencies), neglecting the $\Lambda_b \to \Lambda_c^+ \pi^-$ and $B_s^0 \to D_s^- \pi^+$ backgrounds in the $B^0 \to D^- \pi^+$ fits, and the limited accuracy of the trigger simulation. Even though the ratio of efficiencies is statistically consistent with unity, the maximum deviation is conservatively assigned as a systematic uncertainty. The difference in interaction probability between kaons and pions is estimated by using Monte Carlo simulation. The systematic uncertainty due to possible discrepancies between the data and simulation is expected to be negligible, and it is not taken into account. The efficiency of the nonresonant D_s decays varies across the Dalitz plane but has a negligible effect on the total $B_s^0 \to D_s^- \pi^+$ efficiency. The sources of systematic uncertainty are summarized in Table I.

TABLE I. Experimental systematic uncertainties for the $\mathcal{B}(B^0 \to D^- K^+)$ and the two f_s/f_d measurements.

	$\mathcal{B}(B^0 \to D^- K^+)$	f_s/f_d
PID calibration	2.5%	1.0%/2.5%
Fit model	2.8%	2.8%
Trigger simulation	2.0%	2.0%
$\mathcal{B}(B^0 \to D^- \pi^+)$	4.9%	
$\mathcal{B}(D_s^+ \to K^+ K^- \pi^+)$		4.9%
$\mathcal{B}(D^+ \to K^- \pi^+ \pi^+)$		2.2%
τ_{B_s}/τ_{B_d}		1.5%

The efficiency corrected ratio of $B^0 \to D^- \pi^+$ and $B^0 \to D^- K^+$ yields is combined with the world average of the $B^0 \to D^- \pi^+$ [5] branching ratio to give

$$\mathcal{B}(B^0 \to D^- K^+) = (2.01 \pm 0.18 \pm 0.14) \times 10^{-4}. \quad (4)$$

The first uncertainty is statistical and the second systematic.

The theoretically cleaner measurement of f_s/f_d uses $B^0 \to D^- K^+$ and $B_s^0 \to D_s^- \pi^+$ and is made according to Eq. (2). By accounting for the exclusive D branching fractions $\mathcal{B}(D^+ \to K^- \pi^+ \pi^+) = (9.14 \pm 0.20)\%$ [13] and $\mathcal{B}(D_s^+ \to K^- K^+ \pi^+) = (5.50 \pm 0.27)\%$ [14], the value of f_s/f_d is found to be

$$f_s/f_d = (0.310 \pm 0.030^{\mathrm{stat}} \pm 0.021^{\mathrm{syst}}) \frac{1}{\mathcal{N}_a \mathcal{N}_F}, \quad (5)$$

where the first uncertainty is statistical and the second is systematic. The statistical uncertainty is dominated by the yield of the $B^0 \to D^- K^+$ mode.

The statistically more precise but theoretically less clean measurement of f_s/f_d uses $B^0 \to D^- \pi^+$ and $B_s^0 \to D_s^- \pi^+$ and is, from Eq. (3),

$$f_s/f_d = (0.307 \pm 0.017^{\mathrm{stat}} \pm 0.023^{\mathrm{syst}}) \frac{1}{\mathcal{N}_a \mathcal{N}_F \mathcal{N}_E}. \quad (6)$$

The two values for f_s/f_d can be combined into a single value, taking all correlated uncertainties into account and using the theoretical inputs accounting for the $SU(3)$ breaking part of the form factor ratio, the nonfactorizable and W-exchange diagram:

$$f_s/f_d = 0.253 \pm 0.017^{\mathrm{stat}} \pm 0.017^{\mathrm{syst}} \pm 0.020^{\mathrm{theor}}. \quad (7)$$

In summary, with 35 pb^{-1} of data collected by using the LHCb detector during the 2010 LHC operation at a center-of-mass energy of 7 TeV, the branching fraction of the Cabibbo-suppressed B^0 decay mode $B^0 \to D^- K^+$ has been measured with better precision than the current world average. Additionally, two measurements of the f_s/f_d production fraction are performed from the relative yields of $B_s^0 \to D_s^- \pi^+$ with respect to $B^0 \to D^- K^+$ and $B^0 \to D^- \pi^+$. These values of f_s/f_d are numerically close to the values determined at LEP and at the Tevatron [4].

We express our gratitude to our colleagues in the CERN accelerator departments for the excellent performance of the LHC. We thank the technical and administrative staff at CERN and at the LHCb institutes and acknowledge support from the National Agencies: CAPES, CNPq, FAPERJ, and FINEP (Brazil); CERN; NSFC (China); CNRS/IN2P3 (France); BMBF, DFG, HGF, and MPG (Germany); SFI (Ireland); INFN (Italy); FOM and NWO (The Netherlands); SCSR (Poland); ANCS (Romania); MinES of Russia and Rosatom (Russia); MICINN, Xuntagal, and GENCAT (Spain); SNSF and SER (Switzerland); NAS Ukraine (Ukraine); STFC (United Kingdom); NSF (USA). We also acknowledge the support received from the ERC under FP7 and the Région Auvergne.

[1] R. Aaij *et al.* (LHCb Collaboration), Phys. Lett. B **699**, 330 (2011).
[2] R. Fleischer, N. Serra, and N. Tuning, Phys. Rev. D **83**, 014017 (2011).
[3] R. Fleischer, N. Serra, and N. Tuning, Phys. Rev. D **82**, 034038 (2010).
[4] D. Asner *et al.*, arXiv:1010.1589.
[5] K. Nakamura *et al.*, J. Phys. G **37**, 075021 (2010).
[6] K. Abe *et al.* (BELLE Collaboration), Phys. Rev. Lett. **87**, 111801 (2001).
[7] A. A. Alves, Jr. *et al.* (LHCb Collaboration), JINST **3**, S08005 (2008).
[8] A. A. Alves, Jr. *et al.* (LHCb Detector at the LHC), JINST **3**, S08005 (2008).
[9] V. V. Gligorov, Report No. LHCb-PUB-2011-003.
[10] M. Williams *et al.*, Report No. LHCb-PUB-2011-002.
[11] A. Hoecker *et al.*, Proc. Sci., ACAT (2007) 040.
[12] T. Skwarnicki, DESY Report No. F31-86-02, 1986.
[13] S. Dobbs *et al.* (CLEO Collaboration), Phys. Rev. D **76**, 112001 (2007).
[14] J. P. Alexander *et al.* (CLEO Collaboration), Phys. Rev. Lett. **100**, 161804 (2008).

R. Aaij,[23] B. Adeva,[36] M. Adinolfi,[42] C. Adrover,[6] A. Affolder,[48] Z. Ajaltouni,[5] J. Albrecht,[37] F. Alessio,[6,37] M. Alexander,[47] G. Alkhazov,[29] P. Alvarez Cartelle,[36] A. A. Alves, Jr.,[22a] S. Amato,[2] Y. Amhis,[38a] J. Amoraal,[23] J. Anderson,[39] R. B. Appleby,[50] O. Aquines Gutierrez,[10a] L. Arrabito,[53] A. Artamonov,[34] M. Artuso,[52,37] E. Aslanides,[6] G. Auriemma,[22a,22b] S. Bachmann,[11] J. J. Back,[44] D. S. Bailey,[50] V. Balagura,[30,37] W. Baldini,[16a] R. J. Barlow,[50] C. Barschel,[37] S. Barsuk,[7] W. Barter,[43] A. Bates,[47] C. Bauer,[10a] Th. Bauer,[23] A. Bay,[38a] I. Bediaga,[1] K. Belous,[34] I. Belyaev,[30,37] E. Ben-Haim,[8] M. Benayoun,[8] G. Bencivenni,[18a] S. Benson,[46] J. Benton,[42] R. Bernet,[39] M.-O. Bettler,[17a,37] M. van Beuzekom,[23] A. Bien,[11] S. Bifani,[12] A. Bizzeti,[17a,17d] P. M. Bjørnstad,[50] T. Blake,[49] F. Blanc,[38a] C. Blanks,[49] J. Blouw,[11] S. Blusk,[52] A. Bobrov,[33] V. Bocci,[22a] A. Bondar,[33] N. Bondar,[29] W. Bonivento,[15a] S. Borghi,[47] A. Borgia,[52] T. J. V. Bowcock,[48] C. Bozzi,[16a] T. Brambach,[9] J. van den Brand,[24] J. Bressieux,[38a] S. Brisbane,[51] M. Britsch,[10a] T. Britton,[52] N. H. Brook,[42] A. Büchler-Germann,[39] A. Bursche,[39] J. Buytaert,[37] S. Cadeddu,[15a] J. M. Caicedo Carvajal,[37] O. Callot,[7] M. Calvi,[20a,20b] M. Calvo Gomez,[35a,35b] A. Camboni,[35a] P. Campana,[18a,37] A. Carbone,[14a] G. Carboni,[21a,21b] R. Cardinale,[19a,19b] A. Cardini,[15a] L. Carson,[36] K. Carvalho Akiba,[23] G. Casse,[48] M. Cattaneo,[37] M. Charles,[51] Ph. Charpentier,[37] N. Chiapolini,[39] X. Cid Vidal,[36] P. E. L. Clarke,[46] M. Clemencic,[37] H. V. Cliff,[43] J. Closier,[37] C. Coca,[28] V. Coco,[23] J. Cogan,[6] P. Collins,[37] F. Constantin,[28] G. Conti,[38a] A. Contu,[51] A. Cook,[42] M. Coombes,[42] G. Corti,[37] G. A. Cowan,[38a] R. Currie,[46] B. D'Almagne,[7] C. D'Ambrosio,[37] P. David,[8] P. N. Y. David,[23] I. De Bonis,[4] S. De Capua,[21a,21b] M. De Cian,[39] F. De Lorenzi,[12] J. M. De Miranda,[1] L. De Paula,[2] P. De Simone,[18a] D. Decamp,[4] M. Deckenhoff,[9] H. Degaudenzi,[38a,37] M. Deissenroth,[11] L. Del Buono,[8] C. Deplano,[15a] O. Deschamps,[5] F. Dettori,[15a,15b] J. Dickens,[43] H. Dijkstra,[37] P. Diniz Batista,[1] D. Dossett,[44] A. Dovbnya,[40] F. Dupertuis,[38a] R. Dzhelyadin,[34] C. Eames,[49] S. Easo,[45] U. Egede,[49] V. Egorychev,[30] S. Eidelman,[33] D. van Eijk,[23] F. Eisele,[11] S. Eisenhardt,[46] R. Ekelhof,[9] L. Eklund,[47] Ch. Elsasser,[39] D. G. d'Enterria,[35a,35c] D. Esperante Pereira,[36] L. Estève,[43] A. Falabella,[16a,16b] E. Fanchini,[20a,20b] C. Färber,[11] G. Fardell,[46] C. Farinelli,[23] S. Farry,[12] V. Fave,[38a] V. Fernandez Albor,[36] M. Ferro-Luzzi,[37] S. Filippov,[32] C. Fitzpatrick,[46] M. Fontana,[10a] F. Fontanelli,[19a,19b] R. Forty,[37] M. Frank,[37] C. Frei,[37] M. Frosini,[17a,17b,37] S. Furcas,[20a] A. Gallas Torreira,[36] D. Galli,[14a,14b] M. Gandelman,[2] P. Gandini,[51] Y. Gao,[3] J-C. Garnier,[37] J. Garofoli,[52] L. Garrido,[35a] C. Gaspar,[37] N. Gauvin,[38a] M. Gersabeck,[37] T. Gershon,[44] Ph. Ghez,[4] V. Gibson,[43] V. V. Gligorov,[37] C. Göbel,[54] D. Golubkov,[30] A. Golutvin,[49,30,37] A. Gomes,[2] H. Gordon,[51] M. Grabalosa Gándara,[35a] R. Graciani Diaz,[35a] L. A. Granado Cardoso,[37] E. Graugés,[35a] G. Graziani,[17a] A. Grecu,[28] S. Gregson,[43] B. Gui,[52] E. Gushchin,[32] Yu. Guz,[34] T. Gys,[37] G. Haefeli,[38a] S. C. Haines,[43] T. Hampson,[42] S. Hansmann-Menzemer,[11] R. Harji,[49] N. Harnew,[51] J. Harrison,[50] P. F. Harrison,[44] J. He,[7] V. Heijne,[23] K. Hennessy,[48] P. Henrard,[5] J. A. Hernando Morata,[36] E. van Herwijnen,[37] W. Hofmann,[10a] K. Holubyev,[11] P. Hopchev,[4] W. Hulsbergen,[23] P. Hunt,[51] T. Huse,[48] R. S. Huston,[12] D. Hutchcroft,[48] D. Hynds,[47] V. Iakovenko,[41] P. Ilten,[12] J. Imong,[42] R. Jacobsson,[37] M. Jahjah Hussein,[5] E. Jans,[23] F. Jansen,[23] P. Jaton,[38a] B. Jean-Marie,[7] F. Jing,[3] M. John,[51]

D. Johnson,[51] C. R. Jones,[43] B. Jost,[37] S. Kandybei,[40] T. M. Karbach,[9] J. Keaveney,[12] U. Kerzel,[37] T. Ketel,[24] A. Keune,[38a] B. Khanji,[6] Y. M. Kim,[46] M. Knecht,[38a] S. Koblitz,[37] P. Koppenburg,[23] A. Kozlinskiy,[23] L. Kravchuk,[32] K. Kreplin,[11] G. Krocker,[11] P. Krokovny,[11] F. Kruse,[9] K. Kruzelecki,[37] M. Kucharczyk,[20a,25] S. Kukulak,[25] R. Kumar,[14a,37] T. Kvaratskheliya,[30,37] V. N. La Thi,[38a] D. Lacarrere,[37] G. Lafferty,[50] A. Lai,[15a] D. Lambert,[46] R. W. Lambert,[37] E. Lanciotti,[37] G. Lanfranchi,[18a] C. Langenbruch,[11] T. Latham,[44] R. Le Gac,[6] J. van Leerdam,[23] J.-P. Lees,[4] R. Lefèvre,[5] A. Leflat,[31,37] J. Lefrançois,[7] O. Leroy,[6] T. Lesiak,[25] L. Li,[3] Y. Y. Li,[43] L. Li Gioi,[5] M. Lieng,[9] R. Lindner,[37] C. Linn,[11] B. Liu,[3] G. Liu,[37] J. H. Lopes,[2] E. Lopez Asamar,[35a] N. Lopez-March,[38a] J. Luisier,[38a] F. Machefert,[7] I. V. Machikhiliyan,[4,30] F. Maciuc,[10a] O. Maev,[29,37] J. Magnin,[1] A. Maier,[37] S. Malde,[51] R. M. D. Mamunur,[37] G. Manca,[15a,15b] G. Mancinelli,[6] N. Mangiafave,[43] U. Marconi,[14a] R. Märki,[38a] J. Marks,[11] G. Martellotti,[22a] A. Martens,[7] L. Martin,[51] A. Martín Sánchez,[7] D. Martinez Santos,[37] A. Massafferri,[1] Z. Mathe,[12] C. Matteuzzi,[20a] M. Matveev,[29] E. Maurice,[6] B. Maynard,[52] A. Mazurov,[32,16a,37] G. McGregor,[50] R. McNulty,[12] C. Mclean,[14a] M. Meissner,[11] M. Merk,[23] J. Merkel,[9] R. Messi,[21a,21b] S. Miglioranzi,[37] D. A. Milanes,[13a,37] M.-N. Minard,[4] S. Monteil,[5] D. Moran,[12] P. Morawski,[25] J. V. Morris,[45] R. Mountain,[52] I. Mous,[23] F. Muheim,[46] K. Müller,[39] R. Muresan,[28,38a] B. Muryn,[26] M. Musy,[35a] P. Naik,[42] T. Nakada,[38a] R. Nandakumar,[45] J. Nardulli,[45] M. Nedos,[9] M. Needham,[46] N. Neufeld,[37] C. Nguyen-Mau,[38a,38b] M. Nicol,[7] S. Nies,[9] V. Niess,[5] N. Nikitin,[31] A. Oblakowska-Mucha,[26] V. Obraztsov,[34] S. Oggero,[23] S. Ogilvy,[47] O. Okhrimenko,[41] R. Oldeman,[15a,15b] M. Orlandea,[28] J. M. Otalora Goicochea,[2] B. Pal,[52] J. Palacios,[39] M. Palutan,[18a] J. Panman,[37] A. Papanestis,[45] M. Pappagallo,[13a,13b] C. Parkes,[47,37] C. J. Parkinson,[49] G. Passaleva,[17a] G. D. Patel,[48] M. Patel,[49] S. K. Paterson,[49] G. N. Patrick,[45] C. Patrignani,[19a,19b] C. Pavel-Nicorescu,[28] A. Pazos Alvarez,[36] A. Pellegrino,[23] G. Penso,[22a,22b] M. Pepe Altarelli,[37] S. Perazzini,[14a,14b] D. L. Perego,[20a,20b] E. Perez Trigo,[36] A. Pérez-Calero Yzquierdo,[35a] P. Perret,[5] M. Perrin-Terrin,[6] G. Pessina,[20a] A. Petrella,[16a,37] A. Petrolini,[19a,19b] B. Pie Valls,[35a] B. Pietrzyk,[4] T. Pilar,[44] D. Pinci,[22a] R. Plackett,[47] S. Playfer,[46] M. Plo Casasus,[36] G. Polok,[25] A. Poluektov,[44,33] E. Polycarpo,[2] D. Popov,[10a] B. Popovici,[28] C. Potterat,[35a] A. Powell,[51] T. du Pree,[23] V. Pugatch,[41] A. Puig Navarro,[35a] W. Qian,[52] J. H. Rademacker,[42] B. Rakotomiaramanana,[38a] I. Raniuk,[40] G. Raven,[24] S. Redford,[51] M. M. Reid,[44] A. C. dos Reis,[1] S. Ricciardi,[45] K. Rinnert,[48] D. A. Roa Romero,[5] P. Robbe,[7] E. Rodrigues,[47] F. Rodrigues,[2] C. Rodriguez Cobo,[36] P. Rodriguez Perez,[36] G. J. Rogers,[43] V. Romanovsky,[34] J. Rouvinet,[38a] T. Ruf,[37] H. Ruiz,[35a] G. Sabatino,[21a,21b] J. J. Saborido Silva,[36] N. Sagidova,[29] P. Sail,[47] B. Saitta,[15a,15b] C. Salzmann,[39] M. Sannino,[19a,19b] R. Santacesaria,[22a] R. Santinelli,[37] E. Santovetti,[21a,21b] M. Sapunov,[6] A. Sarti,[18a,18b] C. Satriano,[22a,22c] A. Satta,[21a] M. Savrie,[16a,16b] D. Savrina,[30] P. Schaack,[49] M. Schiller,[11] S. Schleich,[9] M. Schmelling,[10a] B. Schmidt,[37] O. Schneider,[38a] A. Schopper,[37] M.-H. Schune,[7] R. Schwemmer,[37] A. Sciubba,[18a,18b] M. Seco,[36] A. Semennikov,[30] K. Senderowska,[26] N. Serra,[39] J. Serrano,[6] P. Seyfert,[11] B. Shao,[3] M. Shapkin,[34] I. Shapoval,[40,37] P. Shatalov,[30] Y. Shcheglov,[29] T. Shears,[48] L. Shekhtman,[33] O. Shevchenko,[40] V. Shevchenko,[30] A. Shires,[49] R. Silva Coutinho,[54] H. P. Skottowe,[43] T. Skwarnicki,[52] A. C. Smith,[37] N. A. Smith,[48] K. Sobczak,[5] F. J. P. Soler,[47] A. Solomin,[42] F. Soomro,[49] B. Souza De Paula,[2] B. Spaan,[9] A. Sparkes,[46] P. Spradlin,[47] F. Stagni,[37] S. Stahl,[11] O. Steinkamp,[39] S. Stoica,[28] S. Stone,[52,37] B. Storaci,[23] U. Straumann,[39] N. Styles,[46] S. Swientek,[9] M. Szczekowski,[27] P. Szczypka,[38a] T. Szumlak,[26] S. T'Jampens,[4] E. Teodorescu,[28] F. Teubert,[37] C. Thomas,[51,45] E. Thomas,[37] J. van Tilburg,[11] V. Tisserand,[4] M. Tobin,[39] S. Topp-Joergensen,[51] M. T. Tran,[38a] A. Tsaregorodtsev,[6] N. Tuning,[23] A. Ukleja,[27] P. Urquijo,[52] U. Uwer,[11] V. Vagnoni,[14a] G. Valenti,[14a] R. Vazquez Gomez,[35a] P. Vazquez Regueiro,[36] S. Vecchi,[16a] J. J. Velthuis,[42] M. Veltri,[17a,17c] K. Vervink,[37] B. Viaud,[7] I. Videau,[7] X. Vilasis-Cardona,[35a,35b] J. Visniakov,[36] A. Vollhardt,[39] D. Voong,[42] A. Vorobyev,[29] H. Voss,[10a] K. Wacker,[9] S. Wandernoth,[11] J. Wang,[52] D. R. Ward,[43] A. D. Webber,[50] D. Websdale,[49] M. Whitehead,[44] D. Wiedner,[11] L. Wiggers,[23] G. Wilkinson,[51] M. P. Williams,[44,45] M. Williams,[49] F. F. Wilson,[45] J. Wishahi,[9] M. Witek,[25] W. Witzeling,[37] S. A. Wotton,[43] K. Wyllie,[37] Y. Xie,[46] F. Xing,[51] Z. Yang,[3] R. Young,[46] O. Yushchenko,[34] M. Zavertyaev,[10a,10b] L. Zhang,[52] W. C. Zhang,[12] Y. Zhang,[3] A. Zhelezov,[11] L. Zhong,[3] E. Zverev,[31] and A. Zvyagin[37]

(LHCb Collaboration)

[1]*Centro Brasileiro de Pesquisas Físicas (CBPF), Rio de Janeiro, Brazil*
[2]*Universidade Federal do Rio de Janeiro (UFRJ), Rio de Janeiro, Brazil*
[3]*Center for High Energy Physics, Tsinghua University, Beijing, China*
[4]*LAPP, Université de Savoie, CNRS/IN2P3, Annecy-Le-Vieux, France*
[5]*Clermont Université, Université Blaise Pascal, CNRS/IN2P3, LPC, Clermont-Ferrand, France*

[6]CPPM, Aix-Marseille Université, CNRS/IN2P3, Marseille, France
[7]LAL, Université Paris-Sud, CNRS/IN2P3, Orsay, France
[8]LPNHE, Université Pierre et Marie Curie, Université Paris Diderot, CNRS/IN2P3, Paris, France
[9]Fakultät Physik, Technische Universität Dortmund, Dortmund, Germany
[10a]Max-Planck-Institut für Kernphysik (MPIK), Heidelberg, Germany
[10b]P. N. Lebedev Physical Institute, Russian Academy of Science (LPI RAS), Moscow, Russia
[11]Physikalisches Institut, Ruprecht-Karls-Universität Heidelberg, Heidelberg, Germany
[12]School of Physics, University College Dublin, Dublin, Ireland
[13a]Sezione INFN di Bari, Bari, Italy
[13b]Università di Bari, Bari, Italy
[14a]Sezione INFN di Bologna, Bologna, Italy
[14b]Università di Bologna, Bologna, Italy
[15a]Sezione INFN di Cagliari, Cagliari, Italy
[15b]Università di Cagliari, Cagliari, Italy
[16a]Sezione INFN di Ferrara, Ferrara, Italy
[16b]Università di Ferrara, Ferrara, Italy
[17a]Sezione INFN di Firenze, Firenze, Italy
[17b]Università di Firenze, Firenze, Italy
[17c]Università di Urbino, Urbino, Italy
[17d]Università di Modena e Reggio Emilia, Modena, Italy
[18a]Laboratori Nazionali dell'INFN di Frascati, Frascati, Italy
[18b]Università di Roma La Sapienza, Roma, Italy
[19a]Sezione INFN di Genova, Genova, Italy
[19b]Università di Genova, Genova, Italy
[20a]Sezione INFN di Milano Bicocca, Milano, Italy
[20b]Università di Milano Bicocca, Milano, Italy
[21a]Sezione INFN di Roma Tor Vergata, Roma, Italy
[21b]Università di Roma Tor Vergata, Roma, Italy
[22a]Sezione INFN di Roma La Sapienza, Roma, Italy
[22b]Università di Roma La Sapienza, Roma, Italy
[22c]Università della Basilicata, Potenza, Italy
[23]Nikhef National Institute for Subatomic Physics, Amsterdam, The Netherlands
[24]Nikhef National Institute for Subatomic Physics and Vrije Universiteit, Amsterdam, The Netherlands
[25]Henryk Niewodniczanski Institute of Nuclear Physics Polish Academy of Sciences, Cracow, Poland
[26]Faculty of Physics and Applied Computer Science, Cracow, Poland
[27]Soltan Institute for Nuclear Studies, Warsaw, Poland
[28]Horia Hulubei National Institute of Physics and Nuclear Engineering, Bucharest-Magurele, Romania
[29]Petersburg Nuclear Physics Institute (PNPI), Gatchina, Russia
[30]Institute of Theoretical and Experimental Physics (ITEP), Moscow, Russia
[31]Institute of Nuclear Physics, Moscow State University (SINP MSU), Moscow, Russia
[32]Institute for Nuclear Research of the Russian Academy of Sciences (INR RAN), Moscow, Russia
[33]Budker Institute of Nuclear Physics (SB RAS) and Novosibirsk State University, Novosibirsk, Russia
[34]Institute for High Energy Physics (IHEP), Protvino, Russia
[35a]Universitat de Barcelona, Barcelona, Spain
[35b]LIFAELS, La Salle, Universitat Ramon Llull, Barcelona, Spain
[35c]Institució Catalana de Recerca i Estudis Avançats (ICREA), Barcelona, Spain
[36]Universidad de Santiago de Compostela, Santiago de Compostela, Spain
[37]European Organization for Nuclear Research (CERN), Geneva, Switzerland
[38a]Ecole Polytechnique Fédérale de Lausanne (EPFL), Lausanne, Switzerland
[38b]Hanoi University of Science, Hanoi, Vietnam
[39]Physik-Institut, Universität Zürich, Zürich, Switzerland
[40]NSC Kharkiv Institute of Physics and Technology (NSC KIPT), Kharkiv, Ukraine
[41]Institute for Nuclear Research of the National Academy of Sciences (KINR), Kyiv, Ukraine
[42]H. H. Wills Physics Laboratory, University of Bristol, Bristol, United Kingdom
[43]Cavendish Laboratory, University of Cambridge, Cambridge, United Kingdom
[44]Department of Physics, University of Warwick, Coventry, United Kingdom
[45]STFC Rutherford Appleton Laboratory, Didcot, United Kingdom
[46]School of Physics and Astronomy, University of Edinburgh, Edinburgh, United Kingdom
[47]School of Physics and Astronomy, University of Glasgow, Glasgow, United Kingdom
[48]Oliver Lodge Laboratory, University of Liverpool, Liverpool, United Kingdom
[49]Imperial College London, London, United Kingdom

[50]*School of Physics and Astronomy, University of Manchester, Manchester, United Kingdom*
[51]*Department of Physics, University of Oxford, Oxford, United Kingdom*
[52]*Syracuse University, Syracuse, New York, USA*
[53]*CC-IN2P3, CNRS/IN2P3, Lyon-Villeurbanne, France*[*]
[54]*Pontifícia Universidade Católica do Rio de Janeiro (PUC-Rio), Rio de Janeiro, Brazil*[†]

*Associated member.
†Associated to Universidade Federal do Rio de Janeiro (UFRJ), Rio de Janeiro, Brazil.